Cerebrovascular degradation of TRKB by MMP9 in the diabetic brain

Deepti Navaratna, Xiang Fan, Wendy Leung, Josephine Lok, Shuzhen Guo, Changhong Xing, Xiaoying Wang, and Eng H. Lo

Neuroprotection Research Laboratory, Departments of Radiology, Neurology, and Pediatrics, Massachusetts General Hospital, Harvard Medical School, Charlestown, Massachusetts, USA.

Diabetes elevates the risk for neurological diseases, but little is known about the underlying mechanisms. Brain-derived neurotrophic factor (BDNF) is secreted by microvascular endothelial cells (ECs) in the brain, functioning as a neuroprotectant through the activation of the neurotrophic tyrosine kinase receptor TRKB. In a rat model of streptozotocin-induced hyperglycemia, we found that endothelial activation of MMP9 altered TRKB-dependent trophic pathways by degrading TRKB in neurons. Treatment of brain microvascular ECs with advanced glycation endproducts (AGE), a metabolite commonly elevated in diabetic patients, increased MMP9 activation, similar to in vivo findings. Recombinant human MMP9 degraded the TRKB ectodomain in primary neuronal cultures, suggesting that TRKB could be a substrate for MMP9 proteolysis. Consequently, AGE-conditioned endothelial media with elevated MMP9 activity degraded the TRKB ectodomain and simultaneously disrupted the ability of endothelium to protect neurons against hypoxic injury. Our findings demonstrate that neuronal TRKB trophic function is ablated by MMP9-mediated degradation in the diabetic brain, disrupting cerebrovascular trophic coupling and leaving the brain vulnerable to injury.

Introduction

Accelerated neurodegeneration and diminished cognitive abilities, learning, and memory are reported in patients with diabetes (1–3). Population-based studies have found an association between diabetes and an increased risk of developing Alzheimer's disease and vascular dementia (4–7). Age-adjusted incidence rates suggest that diabetic patients are 2.9 times more likely to suffer a stroke compared with nondiabetic patients (8–10). However, insight into the mechanisms of injury is lacking. How does diabetes confer this elevated risk for neurological injury? Our study provides proof of concept that endothelial upregulation of the matrix metalloproteinase, MMP9, degrades the brain-derived neurotrophic factor (BDNF) receptor TRKB in neurons, and this loss of cerebrovascular trophic coupling may, in part, explain the progressive loss of endogenous neuroprotection in the diabetic brain.

Results and Discussion

In situ zymography showed an upregulation of MMP activity in the cerebrovasculature of 6-week streptozotocin-induced diabetic rat cortex (Figure 1, A and C). To confirm this MMP signal in blood vessels, we performed gelatin zymography on the microvessel-enriched fractions of control and streptozotocin-induced hyperglycemic cortex (Figure 1B). These elevations in MMP9 were far subtler than those found in cerebral ischemia and infarction. Increases in MMP9 were much higher and occurred in neurons as well as in endothelium after stroke (Supplemental Figure 1; supplemental material available online with this article; doi:10.1172/JCI65767DS1). A significant increase in MMP9 protein levels was seen in the 6- and 12-week diabetic cerebrovasculature (Figure 1D); no changes in MMP2 were observed.

Vascular dysfunction in diabetes is most commonly associated with elevations in advanced glycation endproducts (AGEs). Thus, we asked whether increased endothelial MMP9 activity could be related to AGEs in our model systems. We treated primary human brain microvascular endothelial cells (ECs) with AGE-BSA, an established prototype of AGEs in diabetes. After 48 hours of AGE stimulation, conditioned medium collected from cells was subjected to gelatin zymography. Treatment with AGE-BSA (0–200 μg/ml) induced a dose-dependent increase in endothelial levels of MMP9 (Figure 1E). Treatment with nonglycated BSA (100 μg/ml) alone did not increase MMP9, suggesting that the response was specific to glycated BSA (Figure 1, F and G). AGE-induced MMP9 appeared to operate via the RAGE receptor, since blockade with an anti-RAGE antibody negated the response (Figure 1H).

Furthermore, we found that AGE-induced MMP9 release was associated with specific endothelial signaling responses. Treatment with AGE-BSA caused a concomitant increase in endothelial phospho-ERK (pERK), along with increased MMP9 secretion into conditioned medium (Figure 1I). Blockade of ERK signaling with an MEK inhibitor (U0126, 5 μM) prevented the AGE-induced MMP9 response (Figure 1J).

Taken together, our findings demonstrate that cerebrovascular MMP9 could be upregulated in the diabetic brain by AGE-driven mechanisms. But how does this lead to increased neuronal vulnerability? We (11) and others (12) previously showed that brain ECs were an important source of neuroprotective BDNF, acting through the TRKB receptor on neurons. So we asked whether MMP9 can disrupt cerebrovascular trophic coupling by degrading neuronal TRKB. We performed TRKB immunostaining on 6-week diabetic and normal rat brain sections. In normal brain, as expected, we found that TRKB was located around neuronal cell bodies and along cortical processes throughout the cortex (Figure 2A). In the 6-week diabetic cortex, TRKB signals appeared to be decreased compared with normal sections (Figure 2A). To examine whether this loss of TRKB signal can indeed be caused by MMP9, we treated normal rat brain sections with recombinant human MMP9 (rhMMP9) (1 μg/ml) prior to probing with TRKB

Conflict of interest: The authors have declared that no conflict of interest exists.

Citation for this article: *J Clin Invest.* 2013;123(8):3373–3377. doi:10.1172/JCI65767.

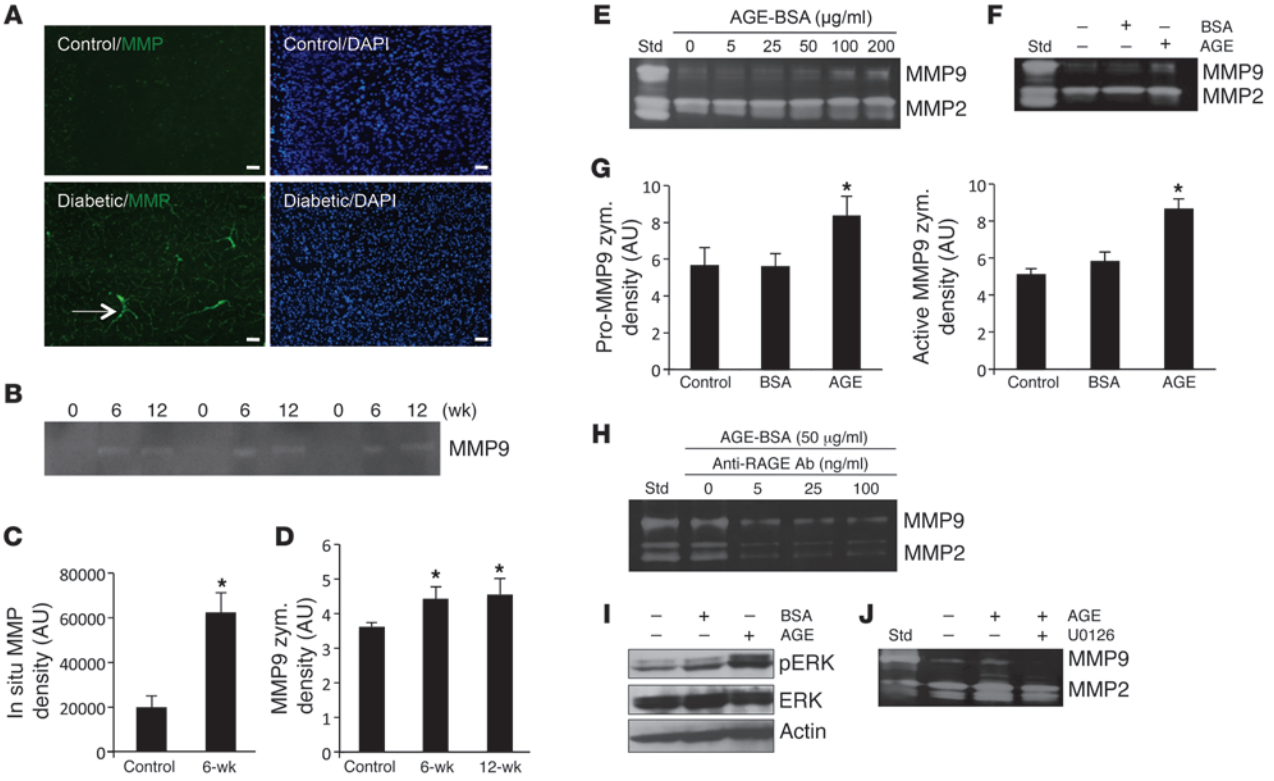

Figure 1

Cerebrovascular MMP9 is upregulated in diabetes. (**A**) Representative in situ zymograms of brain sections from 6-week diabetic and age-matched nondiabetic rats. Scale bars: 100 μm. (**B**) Representative zymogram showing increased MMP9 in microvessel-enriched fractions in 6-week diabetic rat cortex. (**C** and **D**) Quantification of MMP9 levels after in situ zymography and gelatin zymography of microvessel-enriched fractions, respectively. *$P < 0.05$ between control and diabetic rat sections; $n = 4$ per group. Error bars indicate SEM. (**E**) Representative zymogram showing a dose-dependent increase in MMP9 after AGE treatment (0–200 μg/ml). (**F**) Representative zymogram showing that exposure to 50 μg/ml AGE-BSA increased MMP9 secretion, while nonglycated BSA did not. (**G**) Densitometric analysis of zymogram (zym.) showing that AGE-BSA significantly increased pro- and active MMP9 compared with untreated cells or cells treated with normal BSA. *$P < 0.05$ between untreated and AGE-BSA treatment; $n = 3$ per group. Error bars indicate SEM. (**H**) Representative zymogram showing that the ability of AGE-BSA to upregulate endothelial MMP9 is blocked by anti-RAGE antibodies. (**I**) Representative Western blot shows increased pERK in cells exposed to AGE-BSA for 48 hours. (**J**) Representative zymogram shows that U0126 (5 μM) prevents the AGE-BSA–induced increase in MMP9. Std, standard.

antibody. The MMP9-treated sections displayed reduced TRKB signals, similar to what was observed in the diabetic sections, suggesting that an MMP-dependent mechanism might be operating in vivo (Figure 2A). To confirm whether TRKB is degraded by MMP9 in vivo, we probed for proteolytic fragments of TRKB processing in whole-brain extracts by Western blotting. An approximately 25-kDa fragment was detected in normal brain extracts in addition to full-length TRKB (Figure 2B). A significant increase in the levels of this fragment was observed in the 6-week and 12-week diabetic brain extracts, suggesting an increase in MMP-dependent TRKB processing (Figure 2, B and C).

To further test this hypothesis, we incubated a TRKB/Fc human chimera with increasing amounts of active rhMMP9 (0.1–1 μm/ml) at 37°C for 2 hours. Heat-inactivated rhMMP9 was used as a control for nonenzymatic effects of the purified MMP9 protein. The TRKB/Fc human chimera contains the whole extracellular domain of human TRKB fused to the C-terminal histidine-tagged Fc region of human IgG1 and is used in several studies as a decoy TRKB receptor to inhibit BDNF-related mechanisms. Upon treatment with rhMMP9, a dose-dependent reduction in the TRKB band and a corresponding increase in the approximately 25-kDa cleaved fragment were detected (Figure 2D). Mass spectrometry confirmed that the 25-kDa fragment was part of the TRKB protein (Supplemental Figure 2). The addition of heat-inactivated rhMMP9 did not result in these proteolytic activities (Figure 2D). Treatment of TRKB/Fc with active rhMMP7 did not produce any proteolytic fragments, suggesting that this degradation might be mostly mediated by MMP9 (Figure 2D). Since exogenous recombinant MMP9 can degrade TRKB protein, we next asked whether this is also true with the MMP9 that is present in AGE-stressed ECs. Conditioned medium from AGE-stressed ECs was collected and added to TRKB/Fc, and Western blotting was performed again. Increasing concentrations of AGE-stressed endothelial-conditioned medium appeared to degrade TRKB, and this activity was blocked by the MMP inhibitor BB-94 (Figure 2E). Finally, we asked whether MMP9 degradation of TRKB can occur in cells. A similar 25-kDa fragment was detectable from primary mouse neuronal extracts, which solely express TRKB T1 on day 13. TRKB T1 is an alternatively spliced isoform of TRKB FL, with an extracellular domain identical to that of the full-length isoform. Upon treatment with rhMMP9, a similar dose-dependent decrease in TRKB T1 was detected, along with the appearance of the cleaved fragment (Figure 2F).

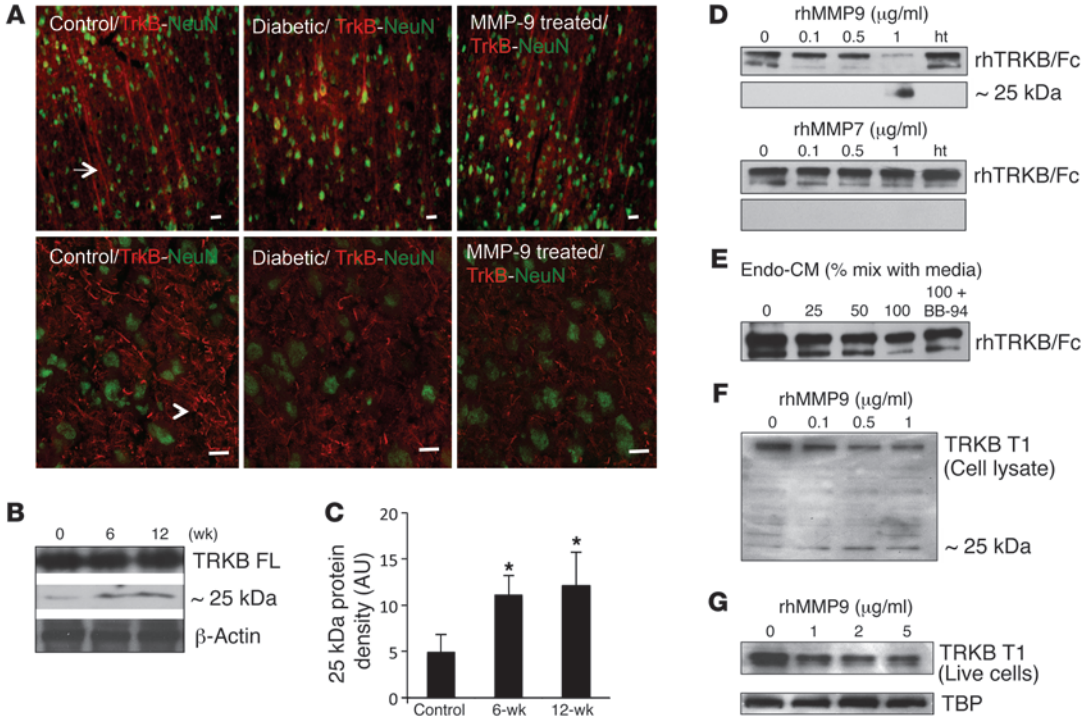

Figure 2

TRKB is degraded by MMP9. (**A**) Representative low-resolution (upper row) and high-resolution (lower row) TRKB immunohistochemistry showing neuronal TRKB signals in normal brains, decreased TRKB in 6-week diabetic rat brain, and decreased TRKB in MMP9-treated normal brain sections. Scale bars: 10 μm. (**B**) Representative Western blot showing increased levels of an approximately 25-kDa fragment in whole-brain extracts from diabetic rats. (**C**) Densitometric quantitation showing that 25-kDa fragments are significantly higher in 6- and 12-week diabetic rat cortex. *$P < 0.05$ between control and diabetic rat cortices; $n = 4$ per group. Error bars indicate SEM. (**D**) rhMMP9 cleaves TRKB/Fc to generate an approximately 25-kDa fragment along with a reduction in the full-length protein. Treatment with heat-inactivated (ht) rhMMP9 or rhMMP7 (0–1 μg/ml) does not generate a similar fragment. (**E**) Conditioned medium (CM) from AGE-stressed ECs (Endo) degrades TRKB/Fc, and this activity was blocked by the MMP inhibitor BB-94. (**F**) rhMMP9 degrades the TRKB T1 isoform in primary mouse embryonic neuronal cell extracts to a similar fragment in a dose-dependent manner (0–1 μg/ml). (**G**) rhMMP9 degrades the TRKB T1 ectodomain in live primary neurons in a dose-dependent manner (0–5 μg/ml).

To confirm whether the ectodomain was indeed accessible for MMP9 cleavage on live cells, we treated primary embryonic mouse neurons with increasing amounts of MMP9 (0–5 μg/ml) in serum-free media. A similar dose-dependent reduction in TRKB T1 was observed (Figure 2G). However, we were unable to detect the shed ectodomain fragment in the conditioned media, possibly because the fragment was further degraded or fragment levels were below blotting efficacy in the conditioned media of our neuronal cultures.

Thus far, our results suggest that elevated MMP9 from diabetic endothelium may degrade TRKB on neurons. To test whether this MMP-mediated TRKB degradation affects neuronal viability, media transfer experiments between brain ECs and primary neuronal cultures were performed (Figure 3A). First, we confirmed that our reagents, AGE-BSA and BB-94, had no direct effects on neuronal viability (Supplemental Figure 3). Then brain endothelial–conditioned medium was added to primary mouse neurons that were subjected to hypoxia for 24 hours. Hypoxia-killed neurons and conditioned medium from normal healthy brain ECs significantly reduced hypoxic neuronal death (Figure 3B), in part by suppressing caspase-3 (Supplemental Figure 4). This protection was dependent on BDNF, since cotreatment with TRKB/Fc negated the neuroprotection (Figure 3B). ELISAs showed that in our models, brain ECs produced approximately 100 pg/ml of BDNF. These BDNF levels were neurobiologically active; 100 pg/ml of exogenous BDNF protected against hypoxia (Supplemental Figure 5) and promoted neurite growth in primary neurons (Supplemental Figure 6). Having established that BDNF from normal brain ECs could protect neurons, we next asked whether MMP9 from AGE-stressed endothelium would degrade TRKB and negate this neuroprotection. Conditioned medium from normal brain ECs significantly reduced hypoxic neuronal death (Figure 3C and Supplemental Figure 7). In contrast, conditioned medium from AGE-BSA–treated ECs was no longer neuroprotective (Figure 3C and Supplemental Figure 7). The addition of the MMP inhibitor BB-94 (25 μM) restored the ability of AGE-BSA–treated ECs to protect against hypoxia (Figure 3C). Similarly, blockade of ERK signaling with U0126 not only prevented MMP9 production in AGE-BSA–treated cells, but also restored the neuroprotective capabilities of AGE-BSA–treated endothelial-conditioned medium (Figure 3D). Taken together, these findings suggest that the ability of brain ECs to protect neurons may be lost in diabetic brains because of disrupted trophic coupling, i.e., upregulated endothelial MMP9 degrades TRKB receptors on neurons (Figure 3E).

Our observations support the possibility that loss of cerebrovascular trophic coupling in diabetes may progressively increase the

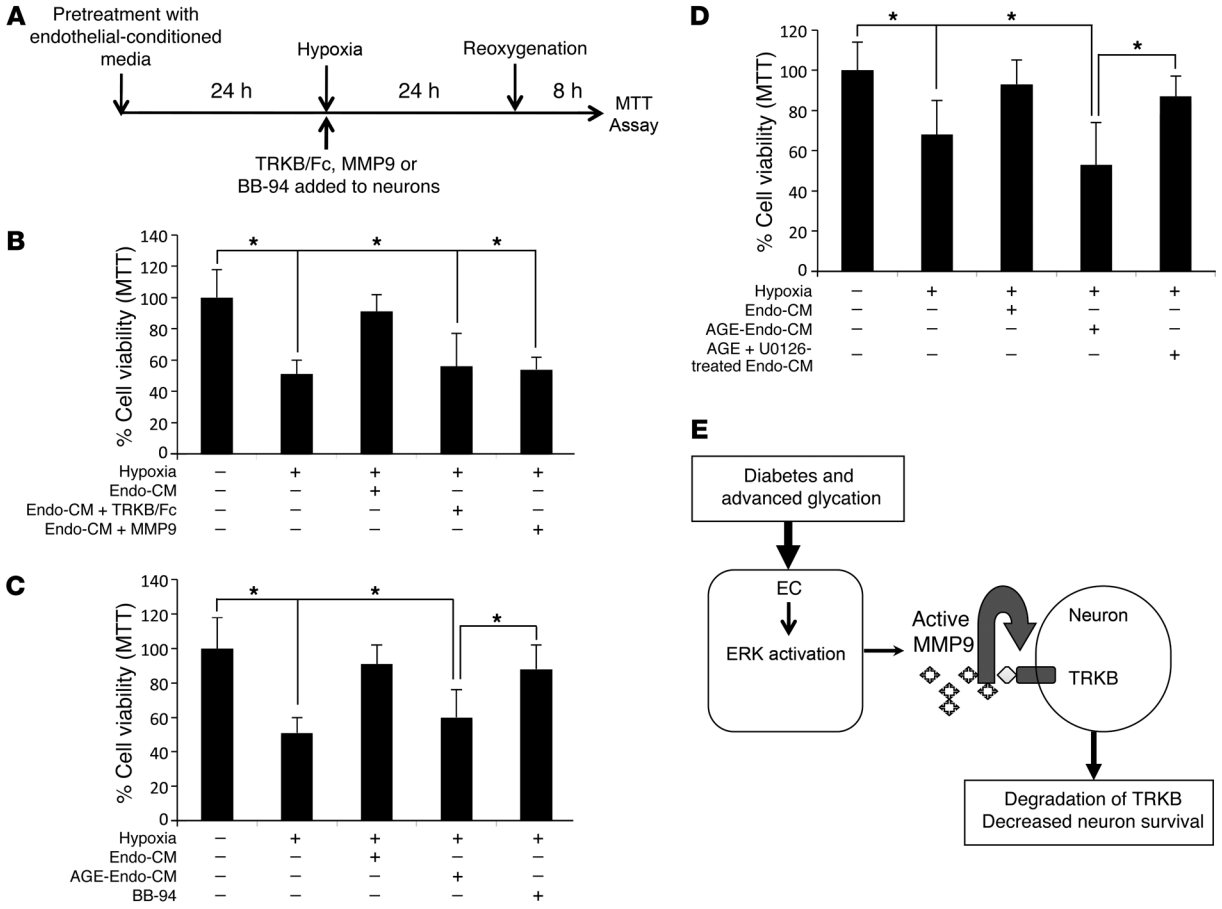

Figure 3

Proteolytic degradation of TRKB by MMP9 leads to decreased cerebrovascular neuroprotection. (**A**) Design of media transfer experiments. (**B**) MTT assays of neuronal viability. Conditioned medium from normal ECs protected primary mouse neurons against 24-hour hypoxia. Conditioned medium from AGE-stressed endothelium was not neuroprotective. Neuroprotection was also negated by the addition of TRKB/Fc or exogenous MMP9. *$P < 0.05$ versus normal neurons; $n = 4$. Error bars indicate SEM. (**C**) MTT assays of neuronal viability. Compared with normal ECs, conditioned medium from AGE-stressed endothelium was not neuroprotective. Neuroprotection was restored by blocking MMP9 with BB-94. *$P < 0.05$ versus normal neurons; $n = 4$. Error bars indicate SEM. (**D**) MTT assays of neuronal viability show that the neuroprotective capability of AGE-stressed endothelial-conditioned medium is restored by blocking ERK signaling with U0126. *$P < 0.05$; $n = 5$ per group. (**E**) Overall model and hypothesis.

risk of neurodegeneration. Vascular enrichment of proteinases in diabetes perhaps has quiescent yet long-ranging effects in diabetic stroke: a higher incidence of microhemorrhages, elevated lacunar stroke with recursive hemorrhagic episodes, and even increased hemorrhagic risk after TPA therapy (9). TRKB ectodomain processing by MMP9 may be consistent with a novel mechanism in which neurotrophic receptor function is possibly regulated by local proteolytic activity. Of course, parallel mechanisms may also exist, including enhanced internalization of TRKB and other receptors in the metabolically perturbed diabetic brain. Nevertheless, a growing list of CNS molecules are emerging as substrates for MMPs, such as β-dystroglycan, zona occludens-1, and myelin basic protein (13). A selective increase or decrease in cell surface presentation of truncated receptors, internalization of ligand-bound receptors, and stimulus-dependent TRKB processing by agents such as zinc are some known pathways through which BDNF is trapped, salvaged, or scavenged (14, 15). Such mechanisms may predominate in situations requiring a rapid and reversible alteration of TRKB on neurons. Proteolytic modification could be another mechanism that disrupts constitutive TRKB dynamics in diseased brain. Chronic activation of cerebrovascular MMP9 and TRKB degradation in diabetes could be responsible for long-term TRKB insufficiency in neurons. Coupled with a lack of trophic support from dysfunctional vasculature, neurons would then be continually unable to respond to available neurotrophic support or compensatory growth factor secretion in affected brain. This hypothesis should eventually be tested in many other models of hyperglycemia, diabetes, and metabolic disease.

In summary, these studies provide proof of concept that in diabetic brains, cerebrovascular upregulation of MMPs may degrade TRKB integrity in neurons, thus potentially disrupting trophic coupling and increasing vulnerability to stroke and neuronal injury.

Methods

Streptozotocin rat model of diabetes. Diabetes was induced with standard streptozotocin (STZ) injections (57.5 mg/kg body weight). Induction of diabetes was verified after 3 days, and rats with blood glucose concentrations greater than 250 mg/dl were included (see Supplemental Methods for details).

Brain microvessel preparation by dextran gradient centrifugation. Brains were collected after PBS perfusion. Cortical gray matter was dissected and rolled on filter paper to remove the large blood vessels, then homogenized with PBS and centrifuged. After washing with PBS, the pellet was resuspended in 4 volumes of 18% dextran and centrifuged at 1,500 *g* for 20 minutes. The new pellet was saved, and the remaining tissue was reprocessed twice in a similar fashion. All 3 pellets were pooled, washed again with PBS, and lysed in lysis buffer (Cell Signaling Technology) with proteinase inhibitors for immunoblotting. Microvessel-enriched fractions in all experiments were not pooled and were derived from a single animal cortex.

Immunohistochemistry. Whole-brain sections (20-μm thick) were prepared from frozen rat brains, air dried, fixed in ice-cold acetone, blocked with 5% BSA, and probed with anti-TRKB rabbit polyclonal antibody (Santa Cruz Biotechnology Inc.) or anti-NEUN antibody (Millipore)

Cell cultures. Primary human brain microvessel ECs (Cell Systems) were mostly derived from a heterogeneous mix of autopsied human brains obtained within a few hours after death. We used cells between passages 5 and 15 at about 90% confluence. Primary mouse embryonic cortex neurons were seeded on poly-D-lysine–coated plates used for conditioned media transfer experiments between days 8 and 10. All treatments with BSA, AGE-BSA, and the MEK/ERK inhibitor U0126 (Calbiochem) were performed in 1% serum MCDB medium supplemented with L-glutamine and 4.5 g/l D-glucose (see Supplemental Methods for details).

Cytotoxicity and immunoblotting. The MTT assay was used to assess cell death in all experiments with primary embryonic neurons. For immunoblotting, primary antibodies were obtained from Santa Cruz Biotechnology Inc. (anti-TRK rabbit polyclonal antibody) and Abcam (anti-TRK mouse monoclonal antibody) and Promega (total and pERK antibodies). Secondary antibodies were obtained from Pharmacia.

Hypoxia and media transfer experiments. Primary ECs were treated with or without AGE-BSA and with or without U0126 for 48 hours before the conditioned media were transferred to neurons. Conditioned media collected from ECs were transferred to primary mouse cortical neurons cultured overnight in serum-free neurobasal media minus B27 and antibiotics. Neurons were then placed in a hypoxic chamber (Billups-Rothenberg). The chamber with cells was perfused with a mixed atmosphere (90% nitrogen, 5% carbon dioxide, and 5% hydrogen) for 30 minutes, and then sealed and placed at 37°C for indicated periods (Figure 3A). After 48 hours, the cells were removed from the chamber, placed in fresh neurobasal serum-free media, and then maintained in a regular CO_2 incubator for reoxygenation. Control cultures were incubated under normoxic conditions for equivalent durations. In some experiments, rhMMP9 or BB-94 was added 2 hours before the neurons were subjected to hypoxia in conditioned media from untreated ECs.

In situ zymography. Sections (20-μm) were cut on a cryostat and incubated at room temperature overnight in 0.05 M Tris-HCl, 0.15 M NaCl, 5 mM $CaCl_2$, and 0.2 mM NaN_3, pH 7.6, containing 40 g of FITC-labeled gelatin (Molecular Probes). This method detects regionally specific gelatinolytic activity but does not distinguish between MMP9 and MMP2. Gelatinolysis was detected with a fluorescence microscope.

Gel zymography. Prepared protein samples were loaded and separated by 10% Tris-glycine gel with 0.1% gelatin as a substrate (Invitrogen). After separation by electrophoresis, the gel was renatured and then incubated with developing buffer at 37°C for 24 hours. After developing, the gel was stained with 0.5% Coomassie blue R-250 for 30 minutes and destained appropriately.

Statistics. A 2-tailed Student's *t* test was performed for 2-group comparisons. One-way ANOVA was performed for multiple-group comparisons, followed by Tukey-Kramer tests for pairwise comparisons. $P < 0.05$ was considered statistically significant.

Study approval. All studies were approved by the IACUC of Massachusetts General Hospital and were conducted in accordance with NIH guidelines for the care and use of laboratory animals.

Acknowledgments

This work was supported in part by NIH grants (R01-NS76694, RC2-NS69335, P01-NS55104), an American Heart Founders Postdoctoral Fellowship, and the Rappaport Foundation.

Received for publication July 11, 2012, and accepted in revised form May 16, 2013.

Address correspondence to: Eng H. Lo or Deepti Navaratna, Neuroprotection Research Laboratory, MGH East 149-2401, 13th Street, Charlestown, Massachusetts 02129, USA. Phone: 617.726.4043; Fax: 617.726.7830; E-mail: Lo@helix.mgh.harvard.edu (E.H. Lo), deeptinavaratna@gmail.com (D. Navaratna).

1. Brands AM, Biessels GJ, de Haan EH, Kappelle LJ, Kessels RP. The effects of type 1 diabetes on cognitive performance: A meta-analysis. *Diabetes Care*. 2005;28(3):726–735.
2. Stewart R, Liolitsa D. Type 2 diabetes mellitus, cognitive impairment and dementia. *Diabet Med*. 1999;16(2):93–112.
3. Allen KV, Frier BM, Strachan MW. The relationship between type 2 diabetes and cognitive dysfunction: Longitudinal studies and their methodological limitations. *Eur J Pharmacol*. 2004;490(1–3):169–175.
4. Ott A, Stolk RP, van Harskamp F, Pols HA, Hofman A, Breteler MM. Diabetes mellitus and the risk of dementia: the Rotterdam Study. *Neurology*. 1999; 53(9):1937–1942.
5. Qiu C, Kivipelto M, Aguero-Torres H, Winblad B, Fratiglioni L. Risk and protective effects of the APOE gene towards Alzheimer's disease in the Kungsholmen project: variation by age and sex. *J Neurol Neurosurg Psychiatry*. 2004;75(6):828–833.
6. Xu WL, Qiu CX, Wahlin A, Winblad B, Fratiglioni L. Diabetes mellitus and risk of dementia in the Kungsholmen project: a 6-year follow-up study. *Neurology*. 2004;63(7):1181–1186.
7. Peila R, Rodriguez BL, Launer LJ, Honolulu-Asia Aging Study. Type 2 diabetes, APOE gene, and the risk for dementia and related pathologies: The Honolulu-Asia Aging Study. *Diabetes*. 2002;51(4):1256–1262.
8. Kissela BM, et al. Epidemiology of ischemic stroke in patients with diabetes: The greater Cincinnati/Northern Kentucky Stroke Study. *Diabetes Care*. 2005;28(2):355–359.
9. Schneider AT, et al. Ischemic stroke subtypes: A population-based study of incidence rates among blacks and whites. *Stroke*. 2004;35(7):1552–1556.
10. Wolf PA, D'Agostino RB, Belanger AJ, Kannel WB. Probability of stroke: A risk profile from the Framingham Study. *Stroke*. 1991;22(3):312–318.
11. Guo S, et al. Neuroprotection via matrix-trophic coupling between cerebral endothelial cells and neurons. *Proc Natl Acad Sci U S A*. 2008;105(21):7582–7587.
12. Dugas JC, Mandemakers W, Rogers M, Ibrahim A, Daneman R, Barres BA. A novel purification method for CNS projection neurons leads to the identification of brain vascular cells as a source of trophic support for corticospinal motor neurons. *J Neurosci*. 2008;28(33):8294–8305.
13. Michaluk P, et al. Beta-dystroglycan as a target for MMP-9, in response to enhanced neuronal activity. *J Biol Chem*. 2007;282(22):16036–16041.
14. Bracken BK, Turrigiano GG. Experience-dependent regulation of TrkB isoforms in rodent visual cortex. *Dev Neurobiol*. 2009;69(5):267–278.
15. Hwang JJ, Park MH, Choi SY, Koh JY. Activation of the trk signaling pathway by extracellular zinc. role of metalloproteinases. *J Biol Chem*. 2005; 280(12):11995–12001.